Available online at www.sciencedirect.com
SCIENCE DIRECT
ELSEVIER
International Journal of Machine Tools & Manufacture 45 (2005) 1375–1385
INTERNATIONAL JOURNAL OF MACHINE TOOLS & MANUFACTURE DESIGN, RESEARCH AND APPLICATION
www.elsevier.com/locate/ijmactool

Modelling the correlation between cutting and process parameters in high-speed machining of Inconel 718 alloy using an artificial neural network

E.O. Ezugwu[a,*], D.A. Fadare[a,b], J. Bonney[a], R.B. Da Silva[a,c], W.F. Sales[a,d]

[a]*Machining Research Centre, Faculty of Engineering, Science and the Built Environment, London South Bank University, 103 Borough Road, London SE1 0AA, UK*
[b]*Department of Mechanical Engineering, Faculty of Technology, University of Ibadan, Ibadan, Nigeria*
[c]*Machining Research and Education Laboratory, Mechanical Engineering Faculty, Federal University of Uberlândia, Uberlândia, MG, Brazil*
[d]*Pontifical Catholic University of Minas Gerais, PUC Minas, Mechanical and Mechatronic Engineering, Manufacturing Research Centre, Belo Horizonte, MG, Brazil*

Received 19 October 2004; accepted 9 February 2005
Available online 25 March 2005

Abstract

An artificial neural network (ANN) model was developed for the analysis and prediction of the relationship between cutting and process parameters during high-speed turning of nickel-based, Inconel 718, alloy. The input parameters of the ANN model are the cutting parameters: speed, feed rate, depth of cut, cutting time, and coolant pressure. The output parameters of the model are seven process parameters measured during the machining trials, namely tangential force (cutting force, F_z), axial force (feed force, F_x), spindle motor power consumption, machined surface roughness, average flank wear (VB), maximum flank wear (VB_{max}) and nose wear (VC). The model consists of a three-layered feedforward backpropagation neural network. The network is trained with pairs of inputs/outputs datasets generated when machining Inconel 718 alloy with triple ($TiCN/Al_2O_3/TiN$) PVD-coated carbide (K 10) inserts with ISO designation CNMG 120412. A very good performance of the neural network, in terms of agreement with experimental data, was achieved. The model can be used for the analysis and prediction of the complex relationship between cutting conditions and the process parameters in metal-cutting operations and for the optimisation of the cutting process for efficient and economic production.

Keywords: Artificial neutral network; Modelling; High-speed turning; Inconel 718 alloy; Elevated temperatures; Optimisation

1. Introduction

Significant advances have recently been made in the field of material science leading to better understanding of the behaviour of engineering materials during processing. This has enabled continual development and introduction of new and novel engineering materials with superior properties and also to a steady increase in the application of new heat-resistant superalloys, such as nickel- and titanium-based alloys in the aerospace industry. The introduction of these materials in the aero-engine has led to a gradual increase of the engine temperature at a rate of 10 °C per annum since the 1950s, resulting in a remarkable increase in engine efficiency and reduction in fuel consumption [1]. These alloys exhibit high strength to weight ratio, high resistance to corrosion, erosion, and wear and are also capable of retaining their mechanical properties such as hardness at elevated temperatures relative to steel and stainless steel alloys [2]. About 70% of the nickel and Ti alloys are usually employed in the aerospace industry for the manufacture of components that demands lighter, harder, stronger, tougher, stiffer, more corrosion- and erosion-resistant materials that are capable of retaining properties at elevated temperatures such as in jet engines. The remainder of these superalloys is widely used in the automobile, chemical, nuclear, medical and construction industry.

The unique and desirable heat-resistant characteristics of superalloys, on the other hand, impair their machinability

* Corresponding author. Fax: +44 171 815 7699.
E-mail address: ezugwueo@sbu.ac.uk (E.O. Ezugwu).

0890-6955/$ - see front matter © 2005 Elsevier Ltd. All rights reserved.
doi:10.1016/j.ijmachtools.2005.02.004

due to the extremely high temperature generated at the cutting edge. This tends to deform the cutting tool, leading to accelerated wear during machining, particularly at higher speed conditions. The machinability aerospace alloys will continue to decline as new materials are developed to meet increasing demand for higher temperature-resistant materials for more efficient aero-engines [1]. Considerable research and development efforts have been directed, worldwide, towards improving the machining operations to ensure efficient and economic machining of these superalloys by proper understanding of the behaviour of exotic superalloys when machining at higher cutting conditions [3].

Advances in cutting tool technology have led to the introduction of coated and uncoated carbide, ceramic, CBN/PCBN and PCD tools with adequate hot hardness and toughness to withstand elevated temperatures generated at high-speed conditions. Also, machining techniques, such as ramping (or taper turning), high-pressure coolant (HPC) delivery system, hot machining, cryogenic machining and the use of self-propelled rotary tooling (SPRT), have been developed in recent years. A good understanding of the behaviour and the relationship between the workpiece materials, cutting tool materials, cutting conditions and the process parameters is an essential requirement for the optimisation of the cutting process. In this regard, a significant number of investigations have been carried out to understand the complex relationship between the cutting conditions and the process parameters in high-speed machining of nickel-based, Inconel 718, alloy from both empirical and theoretical standpoints. Empirical models relating tool wear and component forces as functions of cutting speed and coolant concentration when machining nickel-based, nimonic C-263, alloy with PVD-coated carbide tools have been reported [4]. Similarly, several experimental and analytical studies have been conducted on high-speed machining of nickel-based, Inconel 718, alloy [5–8]. It must be pointed out, however, that these techniques are both costly and time consuming. Computer-based models, on the other hand, offer a more efficient and cost-effective method in modelling the complex process parameters.

Artificial neural networks (ANNs) are one of the most powerful computer modelling techniques, based on statistical approach, currently being used in many fields of engineering for modelling complex relationships which are difficult to describe with physical models. ANNs have been extensively applied in modelling many metal-cutting operations such as turning, milling, and drilling [9–12]. However, this study was inspired by the very limited or no work on the application of ANNs in modelling the relationship between cutting conditions and the process parameters during high-speed machining of nickel-based, Inconel 718, alloy.

2. Model description

There has been continual increase in research interest in the applications of ANNs in modelling and monitoring of machining operations [13,14]. The input/output dataset of the model is illustrated schematically in Fig. 1. The input parameters of the neural network are the cutting conditions, namely cutting speed, feed rate, cutting time and the coolant delivery pressure. The output parameters are seven of the most important process parameters, namely component forces (tangential or cutting force, F_z and axial or feed force, F_x), spindle motor power consumption, machined surface roughness, and tool wear (average and maximum flank wear as well as nose wear).

The five basic steps used in general application of neural network are adopted in the development of the model: assembly or collection of data; analysis and pre-processing of the data; design of the network object; training and testing of the network; and performing simulation with the trained network and post-processing of results.

2.1. Experimentation/collection of input/output dataset

Machining tests were conducted on an 11 kW CNC lathe with a speed range from 18 to 1800 rpm, which provides a torque of 1411 N m. 200 mm diameter and 300 mm long cast solution treated, vacuum inducted melted and electroslag remelted nickel-based, Inconel 718, alloy bars were used as workpiece. The chemical composition and physical properties of the workpiece are given in Tables 1 and 2, respectively. Before conducting the machining trials, up to 3 mm thickness of the top surface of each bar was cleaned in order to eliminate any skin defect that can adversely affect the machining result.

Triple ($TiCN/Al_2O_3/TiN$) PVD-coated carbide (K 10) inserts with ISO designation CNMG 120412412 were used for the machining trials. The physical properties and nominal chemical composition of the inserts are given in Table 3. Cutting conditions, typical of rough turning of nickel-based alloys in the manufacturing industry, employed in the machining trials are shown in Table 4.

During the machining trials, the component forces were measured using a piezo-electric tri-axial dynamometer (Type 9257B). Signals from the dynamometer were

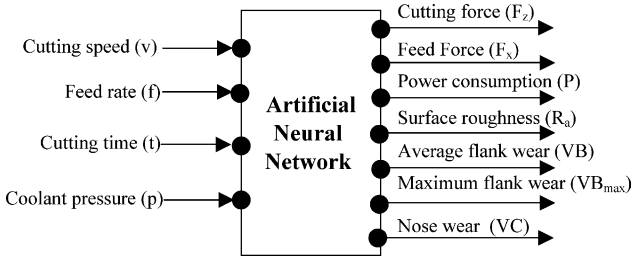

Fig. 1. Schematic model of artificial neural network for prediction of process parameters for Inconel 718 alloy.

Table 1
Chemical composition of Inconel 718 (wt%)

Element	C	Si	Mn	S	Cr	Fe	Mo	Nb and Ta	Ti	Al	Ci	Ni
Wt (%)	0.08	0.35	0.35	0.15	18.6	17.8	3.1	5.0	0.9	0.5	0.3	Balance

Table 2
Physical properties of Inconel 718

Tensile strength (MPa)	Yield strength (MPa)	Elastic modulus (GPa)	Hardness (HRC)	Density (g/cm^3)	Melting point (°C)	Thermal conductivity (W/m K)
1310	1110	206	38	8.19	1300	11.2

Table 3
Chemical and physical properties of coated carbide tool material

Co (vol.%)	WC (vol.%)	TaC (vol.%)	NbC (vol.%)	Hardness (HV)	Grain size (μm)	K1C [MPa (m$^{-1/2}$)]	Coating thickness (μm)		
							TiCN	Al_2O_3	TiN
17.1	81	1.2	0.6	2000	1.7	14	4	1	0.5

conditioned through charge amplifiers (Type 5001) with in-built low-pass filters of 680 Hz cut-off frequency. The RMS values of the signals were sampled at a rate of 200 kHz with a two-channel digital oscilloscope. The power consumption of the spindle motor was measured with a multifunction three-phase power meter. The roughness of the machined surface was measured after each test with a stylus-type instrument. Readings were taken at three different locations and the average value was recorded. Tool wear: average (VB) and maximum (VB_{max}) flank wear, and nose wear (VC) were measured with a travelling microscope connected to a digital readout device at a magnification of ×25.

The tool rejection criteria for roughing operation were used in the machining trials in accordance with ISO Standard 3685. An insert was rejected and further machining discontinued when any or a combination of the following criteria is reached:

- average flank wear ≥ 0.4 mm
- maximum flank wear ≥ 0.7 mm
- nose wear ≥ 0.5 mm
- surface roughness ≥ 6.0 μm

2.2. Pre-processing of input/output dataset

The generalisation capability of the neural network is essentially dependent on: (i) the selection of the appropriate input/output parameters of the system; (ii) the distribution of the dataset; and (iii) the format of the presentation of the dataset to the network. For this model, the input parameters used are the four main cutting parameters, while the output dataset are the seven process parameters. In total, 20 machining tests were conducted and a total of 102 input/output dataset pairs were collected during the machining tests. The experimental design and the data distribution of the input/output dataset for each test are given in Table 4.

Prior to the use of the datasets, principal component analysis was performed, using the Matlab subroutine *prepca*, to test the correlation between the input and output dataset. Result shows that each of the four selected cutting parameters (input dataset) accounts for more than 98% variability in each of the process parameters (output dataset). Before training the network, the input/output datasets were normalised within the range of ±1, using the Matlab subroutine *premnmx*. The normalised value (x_i) for each raw input/output dataset (d_i) was calculated as

$$x_i = \frac{2}{d_{max} - d_{min}}(d_i - d_{min}) - 1$$

Table 4
Cutting parameters

Machining conditions	
Cutting speed (m/min)	20, 30, 40, and 50
Feed rate (mm/rev)	0.25 and 0.30
Depth of cut (mm)	2.0–3.5 (ramping)
Coolant pressure (bar)	110, 150, and 203
Coolant concentration (%)	6.0
Cutting geometry	
Cutting tool insert	CNMG 120412
Tool holder	MSLNR 252512
Approach angle (°)	40.0
Side rake angle (°)	0.0
Clearance angle (°)	6.0
Back rake angle (°)	−5.0
Cutting fluid type	
Emulsion oil (alkanolamine salts of the fatty acids and dicyclohexylamine)	

where d_{max} and d_{min} are the maximum and minimum values of the raw data.

2.3. Neural network design and training

The network architecture or features such as number of neurons and layers are very important factors that determine the functionality and generalisation capability of the network. For this model, standard multilayer feedforward backpropagation hierarchical neural networks were designed with MATLAB 6.1 Neural Network Toolbox [15]. The networks consist of three layers: the input, hidden layer, and output layer. In order to determine the optimal architecture, four different networks with different number of layers and neurons in the hidden layer were designed and tested. In general, the networks have four neurons in the input, corresponding to each of the four cutting parameters and one neuron in the output layer, corresponding to each of the process parameter. Networks with one or two layers and with 10 or 15 in the hidden layer(s) were used as shown in Table 5. For all networks linear transfer function '*purelin*' and tangent sigmoid transfer function '*tansig*' were used in the output and hidden layer, respectively. Seven different networks were designed for each of the process parameters. The networks were trained with Levenberg–Marquardt algorithm. This training algorithm was chosen due to its high accuracy in similar function approximation [3,15]. In order to improve the generalisation of the network, different 'regularisation' schemes were used in conjunction with the Levenberg–Marquardt algorithm. The automatic Bayesian regularisation and the Early stopping regularisation were used (see Table 5).

For training with the Levenberg–Marquardt combined with Bayesian regularisation, the input/output dataset was divided randomly into two categories: training dataset, consisting of two-thirds of the input/output dataset and test dataset, which consists of one-third of the data. When the networks were trained with Levenberg–Marquardt combined with Early stopping, the input/output dataset was divided in three sets: training, test, and validation. One-half of the data was used as training set, one-quarter as test set and one-quarter as validation set.

2.4. Testing and performance of the network

The performance capability of each network was examined based on the correlation coefficient between the network predictions and the experimental values using

Table 5
Correlation coefficient between the network predictions and the experimental values using the training, test and entire dataset for different network and training parameters

Training algorithm/ regularisation	Levenberg–Marquardt with Bayesian regularisation				Levenberg–Marquardt with Early stopping regularisation			
No. of hidden layers	1	1	2	2	1	1	2	2
No. of neurons in the layer	10	15	10	15	10	15	10	15
Surface roughness (Ra)								
Training	0.9551	0.9394	0.9889	0.9849	0.9913	0.9945	0.9965	0.9968
Test	0.9726	0.9535	0.9938	0.9936	0.7728	0.7805	0.7383	0.8224
Entire	0.9566	0.9394	0.9901	0.9870	0.9009	0.9075	0.8990	0.8858
Cutting force (F_z)								
Training	0.5095	0.5094	0.6429	0.6430	0.6706	0.4475	0.6112	0.5626
Test	0.4949	0.4955	0.7164	0.7164	0.4178	0.5031	0.2842	0.2158
Entire	0.5026	0.5027	0.6595	0.6595	0.5509	0.4753	0.4696	0.4204
Feed force (F_x)								
Training	0.7215	0.7069	0.7638	0.7713	0.8363	0.9413	0.8915	0.9225
Test	0.8153	0.7993	0.8666	0.8405	0.3749	0.1686	0.2111	0.2416
Entire	0.7475	0.7345	0.7913	0.7865	0.6593	0.6324	0.6158	0.6323
Power consumption (p)								
Training	0.9664	0.9656	0.9743	0.9748	0.9769	0.9874	0.9686	0.9985
Test	0.9274	0.9443	0.9674	0.9697	0.8805	0.8791	0.9218	0.8827
Entire	0.9571	0.9606	0.9727	0.9735	0.9301	0.9361	0.9426	0.9313
Average flank wear (VB)								
Training	0.9807	0.9810	0.9959	0.9946	0.9851	0.9996	0.9973	1.0000
Test	0.9790	0.9798	0.9982	0.9981	0.8991	0.8953	0.8961	0.9157
Entire	0.9802	0.9804	0.9965	0.9954	0.9352	0.9375	0.9376	0.9415
Maximum flank wear (VB)								
Training	0.9864	0.9877	0.9921	0.9923	0.9776	0.9933	0.9997	1.0000
Test	0.9952	0.9955	0.9980	0.9979	0.9478	0.9262	0.9460	0.9265
Entire	0.9883	0.9894	0.9933	0.9935	0.9512	0.9401	0.9631	0.9439
Nose wear (VC)								
Training	0.9810	0.9817	0.9973	0.9893	0.9880	0.9982	0.9931	0.9935
Test	0.9852	0.9871	0.9980	0.9928	0.9273	0.8905	0.8812	0.9329
Entire	0.9828	0.9838	0.9976	0.9906	0.9569	0.9404	0.9469	0.9466

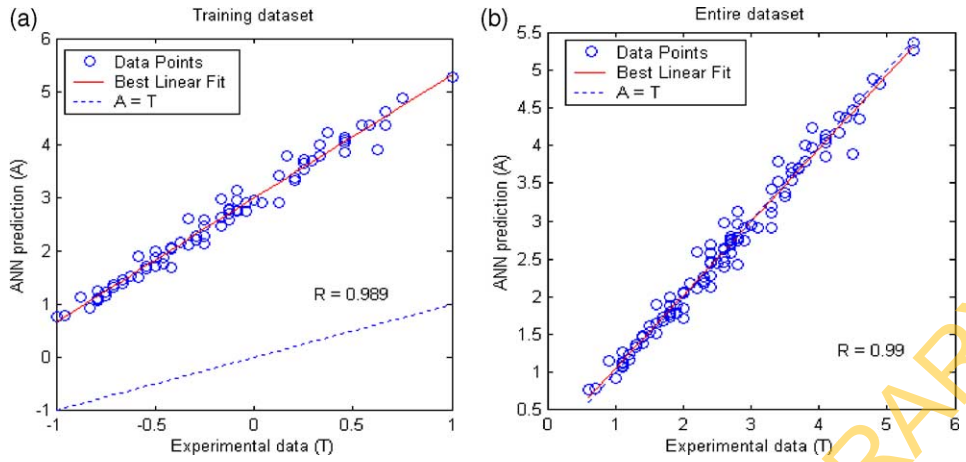

Fig. 2. Correlation between the predicted values of the neural network model and the experimental data for prediction of surface roughness using the training (a) and entire (b) datasets.

the training, test and entire dataset. The best results, obtained from 10 different trials using different random initial weights and biases, for each process parameter are listed in Table 5. Generally, as shown in the table, networks with two hidden layers and 10 neurons in each layer, trained with Levenberg–Marquardt algorithm combined with Bayesian regularisation, gave the best performance for each of the process parameters. It can also be seen that the increase in the number of neurons in the hidden layer from 10 to 15 has no significant improvement on the performance of the networks. Thus, network having two layers and 10 neurons in each hidden layer (4-10-10-1), trained with Levenberg–Marquardt algorithm and Bayesian regularisation, was chosen as the optimum network and used for development of this model. The performance of the model for prediction of surface roughness using the training and entire dataset is shown in Fig. 2. The correlation coefficient of 0.99 was obtained between the entire dataset and the model predictions. The percentage error of the model prediction was also calculated as the percentage difference between the experimental and predicted value relative to the experimental value. The error distribution of the model for the prediction of surface roughness using the entire dataset is shown in Fig. 3. The error has a uniform distribution pattern about zero with a mean value and standard deviation of -0.87 and 7.16%, respectively. The result shows that 84% of the entire dataset have the percentage error ranging between $\pm 10\%$. Acceptable results were also obtained for all the other process parameters. This demonstrated that the models have high accuracy for predicting the process parameters.

3. Simulation and results

3.1. Effect of cutting conditions on the process parameters

Based on the optimised network parameters, ANN model was developed to predict each process parameter based on the cutting conditions, with a high degree of accuracy within the scope of cutting conditions investigated in the study. Thus, the influence of the cutting conditions on the process parameters can be studied using the model.

3.1.1. Effect of cutting speed on the process parameters

Cutting speed is one of the most important cutting parameters in metal-cutting operations. Its influence on the process parameters: surface roughness, cutting force, feed force, power consumption, average flank wear, maximum flank wear, and nose wear over the speed range of 20–50 m/min was examined using the neural network model at constant feed rate of 0.25 mm/rev, coolant pressure of 110 bar and cutting time of 312 s. Results of the neural network predictions and the experimental values are shown in Fig. 4(a)–(g). Fig. 4(a) shows that the predicted surface roughness increased significantly with increasing cutting speed. The deterioration experienced in the machined surface with increase in cutting speed can be attributed to the presence of chatter and tool wear at higher speed conditions. The pattern of the predicted component forces (cutting and feed force) was similar as illustrated in Fig. 4(b)

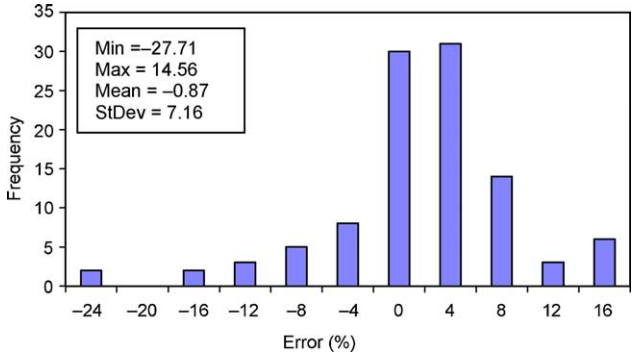

Fig. 3. Error distribution of the neural network model for the prediction of surface roughness using the entire dataset.

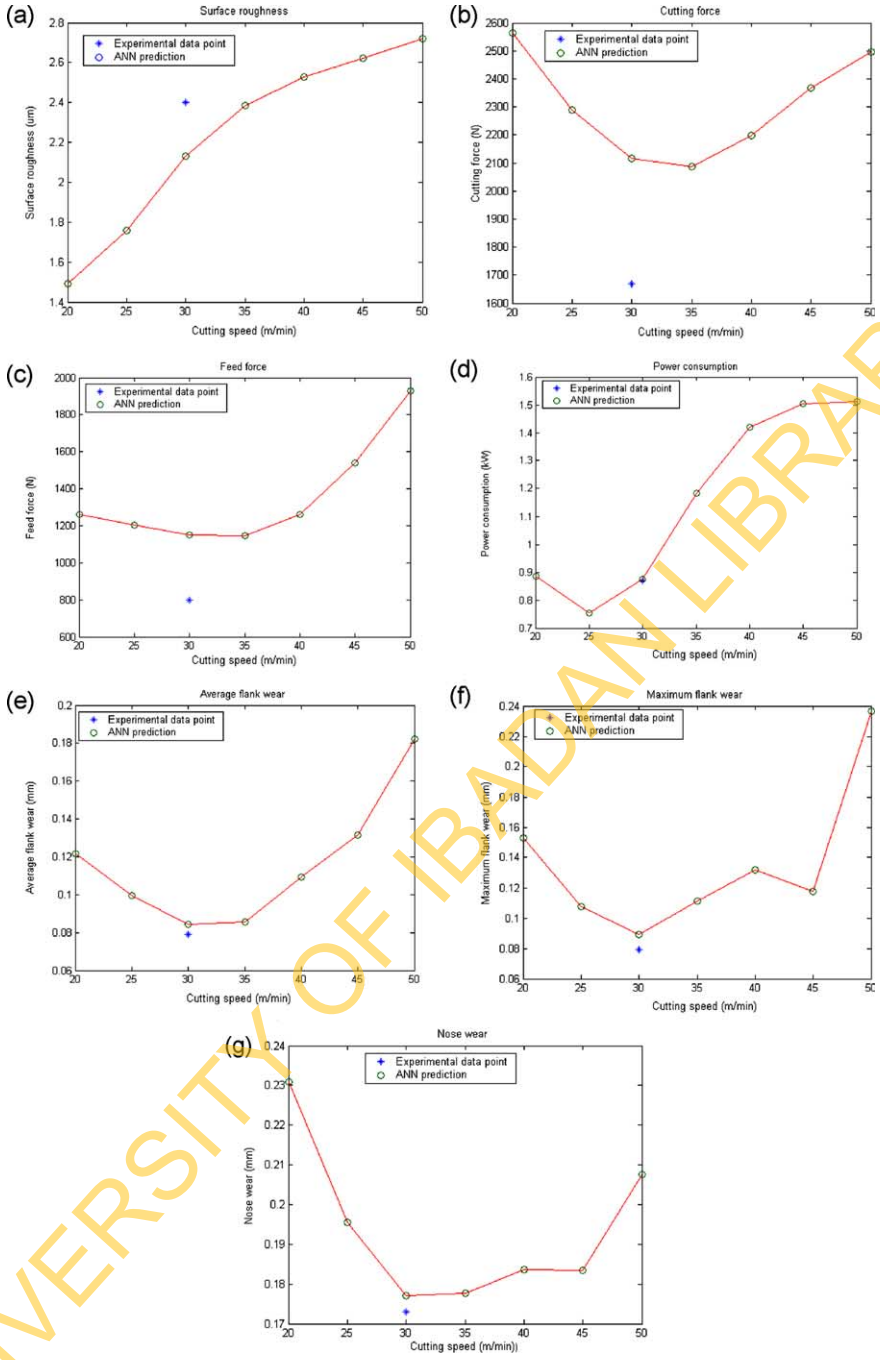

Fig. 4. Neural network prediction of the influence of cutting speed on surface roughness (a), cutting force (b), feed force (c), power consumption (d), average flank wear (e), maximum flank wear (f), and nose wear (g) at constant feed rate of 0.25 mm/rev, coolant pressure of 110 bar and cutting time of 312 s.

and (c). It can be seen that the cutting force reduced significantly (Fig. 4(b)), relative to the feed force (Fig. 4(c)) when the cutting speed increased from 20 to 35 m/min. Further increase in cutting speed, from 35 to 50 m/min, resulted in rapid increase in both cutting and feed forces. The effect of cutting speed on component forces is in two contrasting phenomena. On one hand, as the cutting speed increases, the tool–chip contact length decreases and the temperature at the cutting zone increases, leading to softening of the workpiece material [16]. There is, therefore, a reduction in the shear strength of the workpiece, hence, the drop in component forces [17]. On the other hand, as the cutting speed increases above 30 m/min, tool wear increases (Fig. 4(e)–(g)), consequently increasing the component forces. These, therefore, suggest that the optimum cutting speed is 35 m/min.

Fig. 4(d) shows that the predicted power consumption dropped slightly with increase in cutting speed from 20 to 25 m/min and then increased exponentially with increase in cutting speed from 25 to 50 m/min.

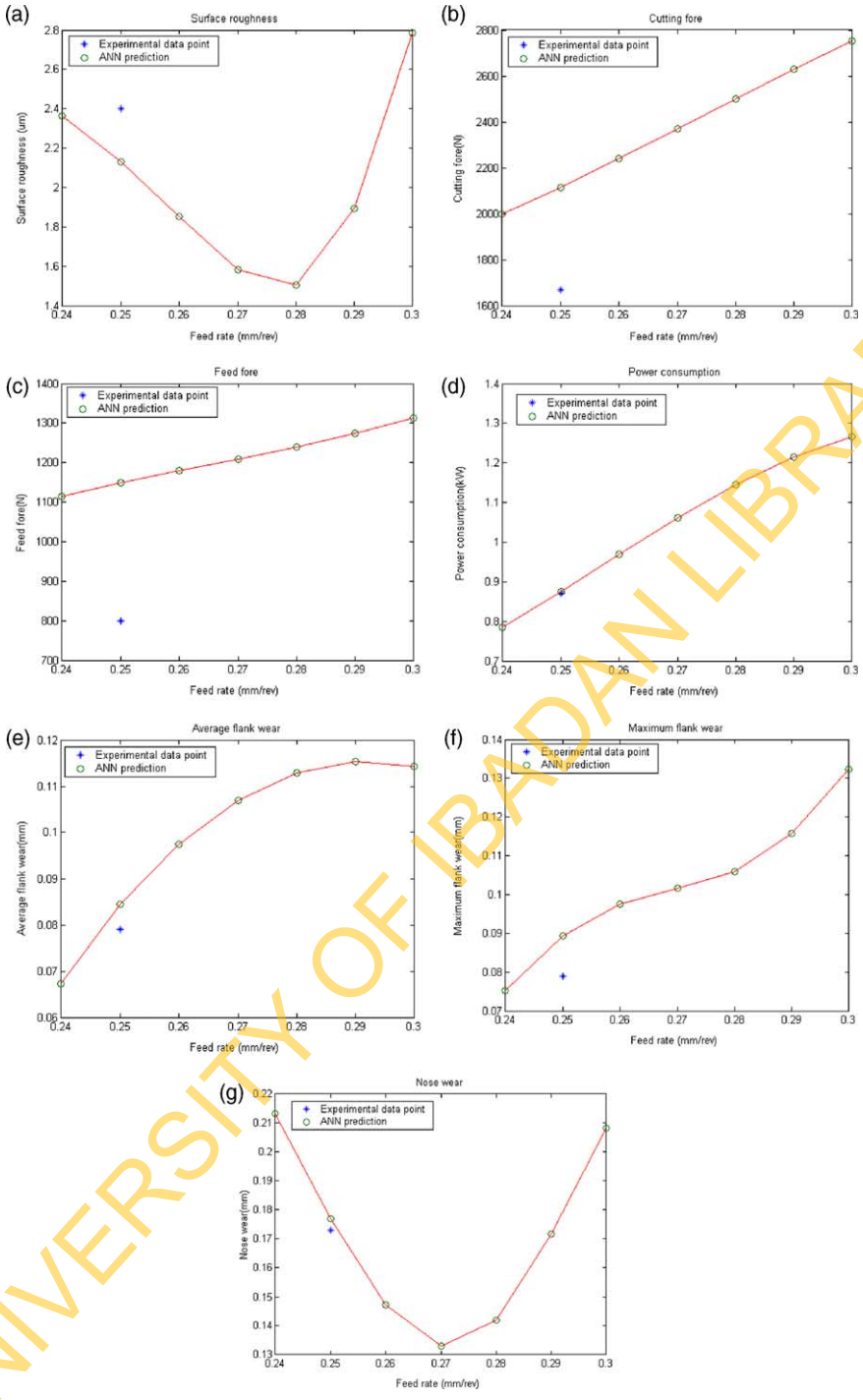

Fig. 5. Neural network prediction of the influence of feed rate on surface roughness (a), cutting force (b), feed force (c), power consumption (d), average flank wear (e), maximum flank wear (f), and nose wear (g) at constant cutting speed of 30 m/min, coolant pressure of 110 bar and cutting time of 312 s.

The trend can then be explained by the corresponding reduction and increase in both component forces and tool wear. In terms of minimum power requirement, the optimum cutting speed is found to be 25 m/min. The predicted tool wear, as shown in Fig. 4(e)–(g), followed a similar pattern. A partially linear reduction in average flank wear (Fig. 4(e)), maximum flank wear (Fig. 4(f)) and nose wear (Fig. 4(g)) was obtained with increase in cutting speed from 20 to 30 m/min. No significant difference was observed in both average flank wear and nose wear unlike gradual increase in the maximum flank wear. Further increase in cutting speed above 35 m/min resulted to a general increase in all the tool wear modes, suggesting that the optimum cutting speed at which minimum process parameters can be obtained is in the range of 25–35 m/min.

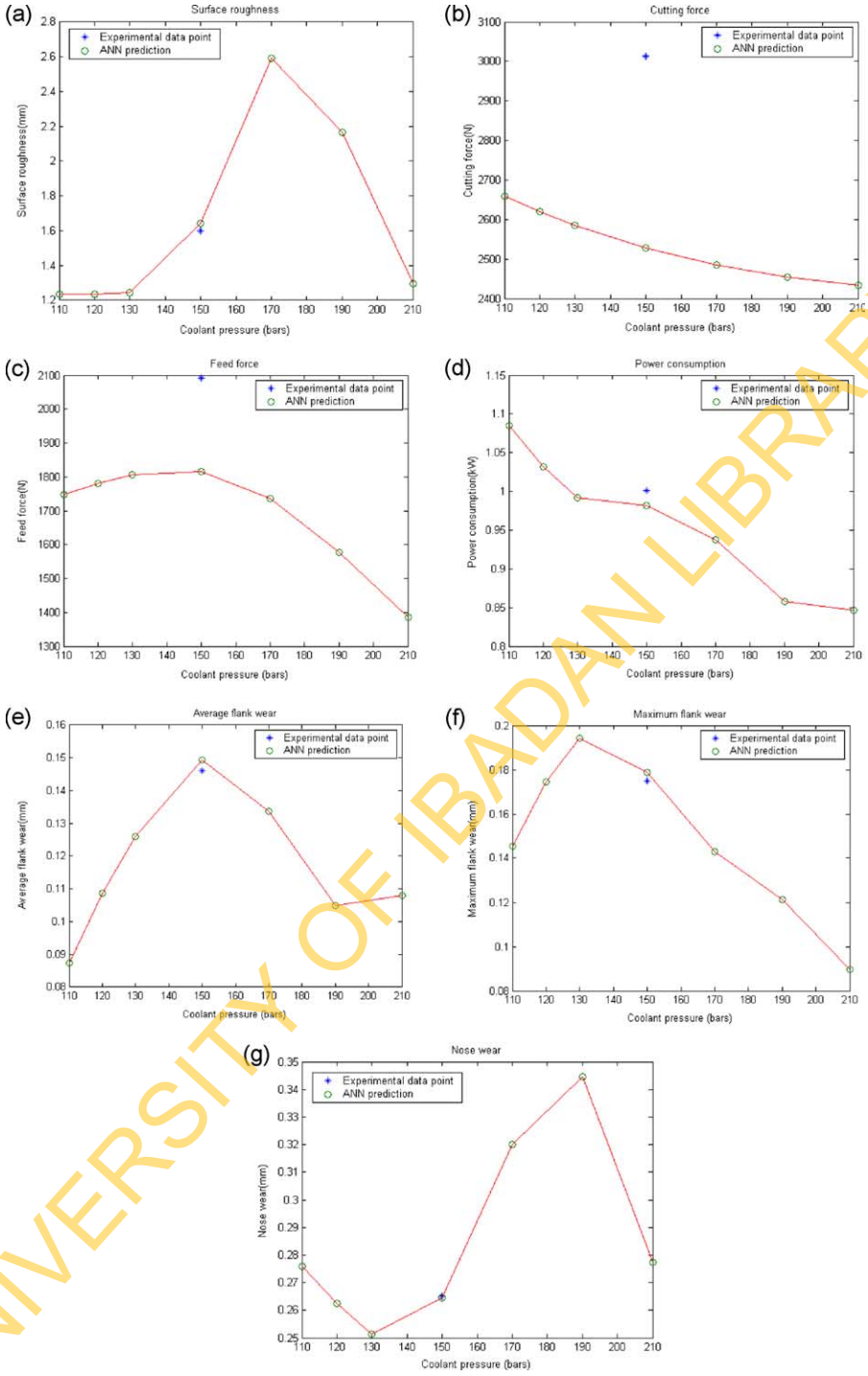

Fig. 6. Neural network prediction of the influence of coolant pressure on surface roughness (a), cutting force (b), feed force (c), power consumption (d), average flank wear (e), maximum flank wear (f), and nose wear (g) at constant cutting speed of 30 m/min, feed rate of 0.25 mm/rev and cutting time of 774 s.

3.1.2. Effect of feed rate on the process parameters

The effects of feed rate on the process parameters are presented in Fig. 5(a)–(g). Fig. 5(a) shows a reduction in the surface roughness value when the feed rate increased from 0.24 to 0.28 mm/rev, contrary to expectation. This reduction can be associated with the corresponding reduction in nose wear with increasing feed rate up to 0.27 mm/rev (Fig. 5(g)). This clearly shows that nose wear has a big influence on the surface roughness generated. Further increase in feed rate above 0.28 mm/rev gave a rapid increase in the surface roughness value. This result indicates that the optimum feed rate is 0.28 mm/rev. An increase in feed rate produces a linear increase in both component forces and the power consumption

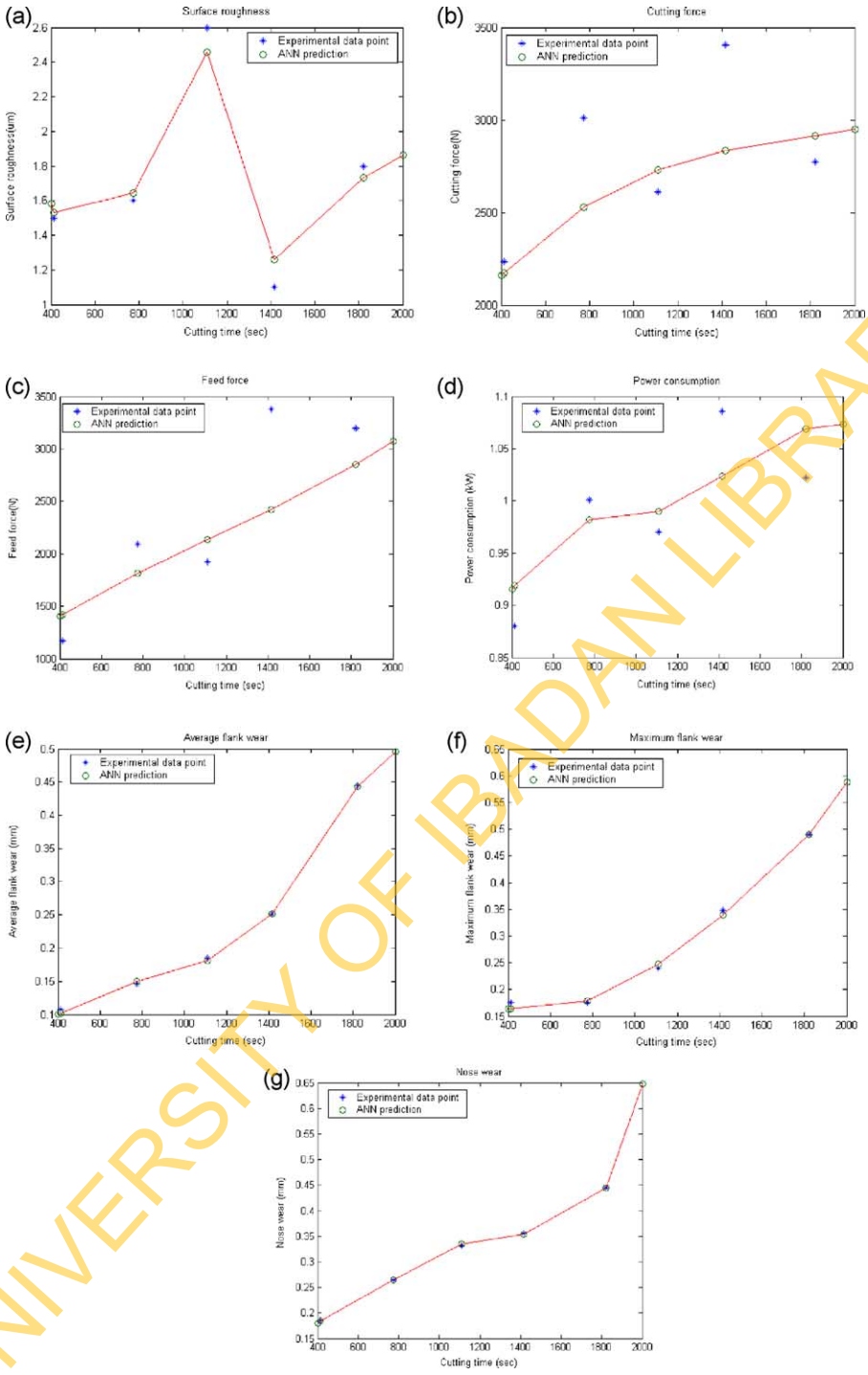

Fig. 7. Neural network prediction of the influence of cutting time on surface roughness (a), cutting force (b), feed force (c), power consumption (d), average flank wear (e), maximum flank wear (f), and nose wear (g) at constant cutting speed of 30 m/min, feed rate of 0.25 mm/rev and coolant pressure of 150 bar.

(Fig. 5(b)–(d)). The average flank wear increased with increase in feed rate up to 0.28 mm/rev, and subsequently levelled off with further increases (Fig. 5(e)), while the maximum flank wear increased steadily with increasing feed rate (Fig. 5(f)). On the other hand, nose wear reduced when the feed rate increased from 0.24 to 0.27 mm/rev and increased with further increase in feed rate (Fig. 5(g)). It can therefore be concluded that the optimum feed rate, corresponding to the minimum surface roughness and nose wear, is within the range of 0.27 and 0.28 mm/rev.

3.1.3. Effect of coolant pressure on the process parameters

The delivery pressure is considered as one of the most important factors in a high-pressure assisted jet cooling

system. The reduction in the temperature at the cutting edge, improvement in tool life and chip breakability achieved with this system depend to a great extent on the delivery pressure [18]. The influence of coolant pressure on the process parameters is shown in Fig. 6(a)–(g). Fig. 6(a) shows that the predicted surface roughness remained constant with increase in coolant pressure from 110 to 130 bar. It then increased with increase in coolant pressure from 130 to 170 bar before dropping rapidly when the pressure increased from 170 to 210 bar. There was a steady reduction in cutting force with increase in pressure (Fig. 6(b)) due probably to reduction in the tool–chip contact length due to the hydraulic wedge created by the HPC jet at tool–chip interface [19]. A slight increase in feed force was obtained when the pressure increased from 110 to 150 bar followed by a rapid reduction when the pressure increased from 150 to 210 bar (Fig. 6(c)). The power consumption dropped steadily with increase in the coolant pressure (Fig. 6(d)), similar to the cutting force. This can also be attributed to the reduction in both tool–chip contact length. Fig. 6(e)–(f) shows the effect of coolant pressure on tool wear. An initial increase was observed in both the average and maximum flank wears with increasing coolant pressure. Further increase in pressure above 150 bar generally lowered the predicted flank wear. An initial reduction in nose wear was obtained with increase in pressure up to 130 bar followed by a steady rise up to 190 bar after which there was a reduction with further increase in pressure from 190 to 210 bar (Fig. 6(g)).

3.1.4. Effect of cutting time on the process parameters

The influence of cutting time on the process parameters is shown in Fig. 7(a)–(g). Fig. 7(a) shows that increase in cutting time has no defined influence on the surface finish generated. Prolonged machining results in steady increase in both component forces, power consumption, average and maximum flank wears, and nose wear as illustrated in Fig. 7(b)–(g).

It is important to note that the experimental values for all the process parameters were very close to the predicted values, except for the predictions of the component forces (Figs. 4(b) and (c)–7(b) and (c)) where the differences were high due to the low correlation coefficient between the measured and the predicted values from the model, which are 0.6595 and 0.7913 for cutting force and feed force, respectively, while that for other process parameters are in excess of 0.9 (Table 5). This shows that the model prediction has a high degree of accuracy.

4. Conclusions

1. The multilayer network with two hidden layers having 10 ‘tangent sigmoid’ neurons trained with Levenberg–Marquardt algorithm combined with Bayesian regularisation was found to be the optimum network for the model developed in this study.
2. A good performance was achieved with the neural model, with correlation coefficient between the model prediction and experimental values ranging from 0.6595 for cutting force to 0.9976 for nose wear prediction.
3. The optimum cutting speed at which minimum process parameters were obtained is in the range of 25–35 m/min, while the optimum feed rate, corresponding to the minimum surface roughness and nose wear, is within 0.27 and 0.28 mm/rev.
4. A consistent reduction in cutting force was achieved with increase in coolant pressure due to reduction in tool–chip contact length as a result of the hydraulic wedge created by the coolant jet at the tool–chip interface. The effect of coolant pressure on tool performance is more pronounced on the maximum flank wear than other wear modes.
5. Prolonged machining results in steady increase in both component forces, power consumption, average and maximum flank wear, and nose wear.

Acknowledgements

One of the authors, D.A. Fadare, is grateful to the John D. and Catherine T. MacArthur Foundation Grant through the University of Ibadan, Nigeria for funding the staff development program during which this study was conducted.

References

[1] E.O. Ezugwu, Advances in the machining of nickel and titanium base superalloys, Keynote paper presented at the Japan Society for Precision Engineering Conference 2004, pp. 1–40.
[2] Seco technical guide, Turning difficulty-to-cut alloys.
[3] S. Malinov, W. Sha, J.J. McKeown, Modelling the correlation between processing parameters and properties in titanium alloys using artificial neural network, Comput. Mater. Sci. 21 (2001) 375–394.
[4] E.O. Ezugwu, K.A. Olajire, J. Bonney, Modelling of tool wear based on component forces, Tribol. Lett. 11 (1) (2001).
[5] E.O. Ezugwu, J. Bonney, Effect of high-pressure coolant supply when machining nickel-base, Inconel 718, alloy with coated carbide tools, Proceedings of AMPT 2003, 8–11 July 2003, Dublin, Ireland, pp. 787–790.
[6] E.O. Ezugwu, J. Bonney, Effect of high-pressure coolant supply when machining nickel-base, Inconel 718, alloy with coated carbide tools, J.Mater. Process. Technol. 153–154 (2004) 1045–1050.
[7] J. Bonney, High-speed machining of nickel-base, Inconel 718, alloy with ceramic and carbide cutting tools using conventional and high-pressure coolants, PhD Thesis, London South Bank University, 2004.
[8] E.O. Ezugwu, A.R. Machado, I.R. Pashby, J. Wallbank, The effect of high-pressure coolant supply when machining a heat-resistant nickel-based superalloy, Lubr. Eng. 47 (9) (1991) 751–757.
[9] E.O. Ezugwu, S.J. Arthur, E.L. Hines, Tool-wear prediction using artificial neural networks, J. Mater. Process. Technol. 49 (1995) 255–264.

[10] T.L. Liu, W.Y. Chen, K.S. Anantharaman, Intelligent detection of drill wear, Mech. Syst. Signal Process. 12 (6) (1998) 863–873.
[11] D.E. Dimla Sr., P.M. Lister, On-line metal cutting tool condition monitoring. II: Tool-state classification using multi-layer perceptron neural networks, Int. J. Mach. Tool Manuf. 40 (2000) 769–781.
[12] D.E. Dimla Sr., Application of perceptron neural networks to tool-state classification in a metal-turning operation, Eng. Appl. Artif. Intell. 12 (1999) 471–477.
[13] B. Sick, On-line and indirect tool wear monitoring in turning with artificial neural networks: a review of more than a decade of research, Mech. Syst. Signal Process. 16 (4) (2002) 487–546.
[14] D.E. Dimla Jr., P.M. Lister, N.J. Leighton, Neural network solution to the tool condition monitoring problem in metal cutting—a critical review of methods, Int. J. Mach. Tools Manuf. 37 (9) (1997) 1219–1241.
[15] H. Demuth, M. Beale, Neural Network Toolbox User's Guide, Version 4 (Release 12), The Mathworks, Inc., 2000.
[16] B. Mills, A.H. Redford, Machinability of Engineering Materials, Applied Science Publishers, Barking, UK, 1983.
[17] X.S. Li, I. Low, Cutting forces of ceramic cutting tools in: X.S. Li, I. Low (Eds.),, Advanced Ceramic Tools For Machining Application—1, Key Engineering Materials vol. 96, Trans Tech Publications, Aedermannsdorf, Switzerland, 1994, pp. 81–136.
[18] C. Richt, Turning Titanium—Developments in Application Technology, Sanvik Coromant, Sandviken, Sweden, 2003.
[19] M. Mazurkiewicz, Z. Kubala, J. Chow, Metal machining with high-pressure water-jet cooling assistance—a new possibility, J. Eng. Ind. 111 (1989) 7–12.